THERMAL EXCHANGES IN A BI-FACIALLY IRRADIATED COLLECTOR INTEGRATED TO AN ADSORPTIVE SOLAR REFRIGERATOR

Antonio Pralon Ferreira Leite
Laboratório de Energia Solar, Universidade Federal da Paraíba
Cidade Universitária, 58059-900 João Pessoa-PB, Brazil
antpralon@yahoo.com.br

Marcelo Bezerra Grilo
Departamento de Engenharia Mecânica, Universidade Federal de Campina Grande
58109-970 Campina Grande-PB, Brazil
margrilo@hotmail.com

Rodrigo Ronelli Duarte de Andrade
Laboratório de Energia Solar, Universidade Federal da Paraíba
Cidade Universitária, 58059-900 João Pessoa-PB, Brazil
rodrigo_ronelli@yahoo.com.br

Francisco Antônio Belo
Laboratório de Energia Solar, Universidade Federal da Paraíba
Cidade Universitária, 58059-900 João Pessoa-PB, Brazil
belo@les.ufpb.br

Francis Meunier
Laboratoire du Froid, Conservatoire National des Arts et Métiers
292, Rue Saint Martin - 75141 Paris Cedex 03, France
meunierf@cnam.fr

Abstract. *This paper analyzes the radiant heat exchanges from an adsorber integrated to an improved bi-facially irradiated collector that is used in a solar-powered refrigerator. The adsorptive pair is the activated carbon-methanol, which is appropriate for ice production. This system works in an intermittent way that consists of a solar energy regeneration stage and a refrigeration adsorption stage, when the intended cooling effect is produced. The solar radiation adsorbing plate is made up of a series of tubes, placed side-by-side, painted in matt black, whose upper and under sides are covered with transparent insulation material (TIM covers). The machine was tested in a Brazilian region close to the Equator (7°8'S, 34°50'WG), over a period of time around the equinox. Based on several data obtained in a typical clear day, we evaluate the net radiant heat flux from the adsorber in the period going from the end of the regeneration and the end of the adsorption. The energy equation for the adsorber is presented, as well as the equations system concerning the thermal radiation transfers between the surfaces around the tubes of the adsorber. The method of resolution is based on the Poljak's model, or the "net-radiation method". Results from calculations have shown that the heat released from the adsorber by radiation corresponds to 75% of the total heat losses, and about 18% of the net radiant flux is due to the interchange between the under side of the tubes and the surrounding surfaces.*

Keywords*: radiant heat exchanges, bi-facial collector, solar refrigeration*

1. Introduction

Solar cooling is one of the most interesting applications of solar energy because the stronger the insolation, the greater needs for cooling. As a rule, the systems requiring thermal energy as their main power input for the production of frigorific effect are most dependable on sorption processes. The use of solar energy for cooling applications is reported more than forty years ago with a device based on the liquid sorption cycle (Chinnappa, 1962). In the last decades, several studies have been made with solar-powered refrigerators based on either a chemical reaction (Spinner et al., 1999) or adsorption (Boubakri, 2003). A comparative study between the three sorption solar cooling systems, i.e., liquid, chemical reaction and adsorption, was published by Meunier (1998). In all these systems the mechanical energy consumption is kept to a minimum or null, i.e. they utilize mainly thermal energy that comes from various sources, as such, process heat, thermal waste or solar energy. This represents a great advantage over the conventional vapor compression systems, especially in countries like Brazil whose energy consumption depends heavily on hydroelectric power.

The adsorption technology applicable to refrigerating systems differs significantly from that of absorption on account of its unsophisticated functioning. In adsorption, there occurs the interaction between a solid and a fluid, the transportation of the latter being thermal gradient dependable, i.e., it does not require the use of pumps. In the case of

liquid absorption cycle, however, a solution interacts with a refrigerating fluid, calling for a number of electromechanical devices in order to move both the solution and the fluid. Moreover, the adsorption cycle depends on fewer electromechanical components (heat exchangers, valves). On the other hand, adsorption refrigeration has shown performance coefficients lower than those obtained by liquid absorption. In the field of solar refrigeration by adsorption, there have been considered various kinds of fluid-solid pairs; zeolite-water (Grenier et al., 1988) and silicagel-water (Hildebrand et al., 2004) are used for cold storage, whereas activated carbon-methanol (Li et al., 2002) and activated carbon-ammonia (Critoph et al., 1997) are used for the production of ice.

This paper presents the heat exchanges from the adsorber-collector of an autonomous solar icemaker calculated from experimental data. The cooling system is based on the adsorption of methanol on activated carbon, and it is viewed for food and vaccine preservation in areas without electricity. The actual adsorptive icemaker prototype utilizes a soft technology for the thermal solar conversion, which is appropriate for a daily intermittent cycle.

2. Adsorption refrigerator

The adsorption icemaker is based on an intermittent cycle, which occurs without heat recovering. This cycle consists of two typical stages: one is characterized by the adsorption process, when the evaporation of the working fluid (the adsorbate) takes place; and another consists of the solid medium (the adsorbent) regeneration by solar energy, when the adsorbate is condensed. The adsorbent-adsorbate pair is the activated carbon-methanol. The solar-powered refrigerator is mainly composed of an integrated adsorber-solar collector, connected to a condenser and an evaporator (Fig. 1). The direction of the gaseous flow is altered, according to the cycle stage; it goes from the adsorber towards the condenser during the regeneration, and from the evaporator towards the adsorber, during the adsorption phase. The TIM covers are in place during regeneration, and retracted otherwise to improve cooling, as shown in Fig. 1.

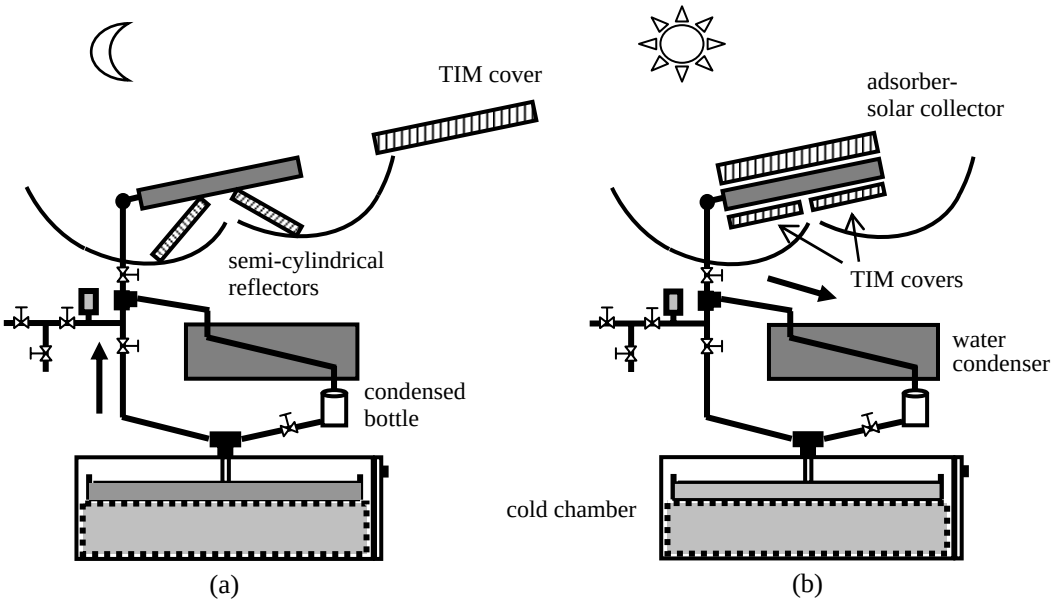

Figure 1. Scheme of the adsorptive icemaker and its operation: (a) Stage of refrigeration; (b) Stage of regeneration.

The refrigeration stage begins by the end of the afternoon, when the temperature and the pressure of the adsorber decrease, following an isosteric process, i.e., a process in which the adsorbed phase concentration (a) is constant. The evaporation takes place when the gaseous adsorbate flows to the adsorber throughout the night, producing the refrigeration effect until the adsorber temperature reaches a minimum value. In another isosteric process (Fig. 1b), the adsorber is heated by the solar radiation incidence, increasing the temperature and pressure until they reach the condenser pressure. Then condensation takes place and the adsorbate is transferred to the condenser until the adsorber reaches a maximum temperature, which means the end of the cycle. The ideal thermodynamic cycle can be represented by two isosters (iso-lines with constant adsorbed phase concentration) and two intercalated isobars, as shown in Fig. 2. Processes 1-2 and 2-3 represent the cooling of the adsorbent and the adsorption, respectively, and processes 3-4 and 4-1 describe the regeneration stage of the adsorbent (heating and desorption). A complete thermodynamic analysis of the adsorption refrigeration system is given by Leite (1998).

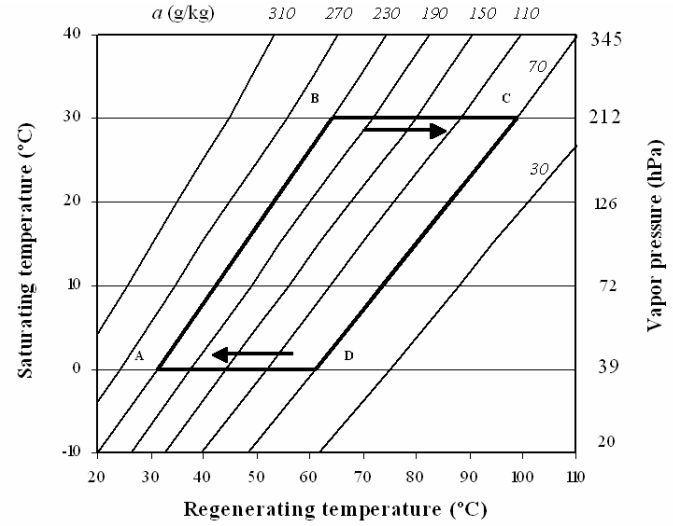

Figure 2. Network of activated carbon-methanol isosters and theoretical cycle.

The dimensioning parameters and a thermal efficiency analysis based on experimental data of the actual prototype have been recently published by Leite et al. (2004, 2005a, 2005b).

2.1 Adsorber-collector.

Since the absorbing plate is a non-selective surface, and in order to improve the collector's efficiency and to obtain temperatures higher than 100°C, the adsorber-collector was covered by a capillary structure in polycarbonate that is mounted between two glass plates, the called TIM covers. Both faces of the adsorber tubes are covered with TIM, and cylindrical reflectors were installed bellow the adsorber. The lower TIM covers are articulated around a central and longitudinal axis, as shown in Fig. 3, while the upper TIM cover is removed by pushing it sideways. The reflectors have a double function: to allow the solar incidence in the lower face of the adsorber, during the regeneration, and to improve its cooling, after the end of the desorption, mainly by means of the longwave radiation exchange with the sky.

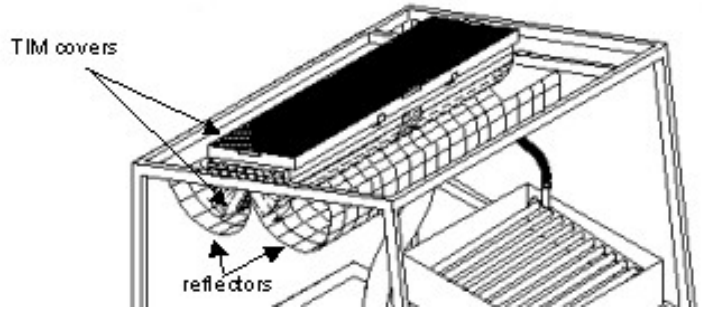

Figure 3. Schematic view of the solar icemaker prototype.

3. Thermal exchanges in the adsorber

A complete analysis about the heat transfers involving the adsorber during the regeneration stage has been made and several results from calculations carried out based on experimental data were recently published (Leite et al., 2005b). We have determined the hourly thermal efficiency by the useful energy method and by the overall heat losses analysis coupled to a graphic model for calculating the optical efficiency. Our results were compared to those from a similar adsorptive machine with a flat adsorber covered by a selective surface and by a single glass plate, and they were very close; both daily thermal efficiencies were around 40%.

The present problem, which is the main objective of this paper, is to evaluate de thermal exchanges from the adsorber, during the period going from the end of the desorption and the end of the adsorption, in order to obtain the net radiant fluxes leaving the adsorber by the upper side and by the under side, which is the energy crossing the aperture surface in the zenith direction. Figure 4 shows the cavity considered for analyzing the radiant heat interchange between the surfaces surrounding the adsorber, which represents the half of the adsorber. Surface 1 corresponds to the tubes (at T_p), surface 2 is the lower TIM cover surface, surface 3 is the reflector, 4 is an opening surface at the sky temperature, and 5 and 6 are opening extremity surfaces at the ambient temperature.

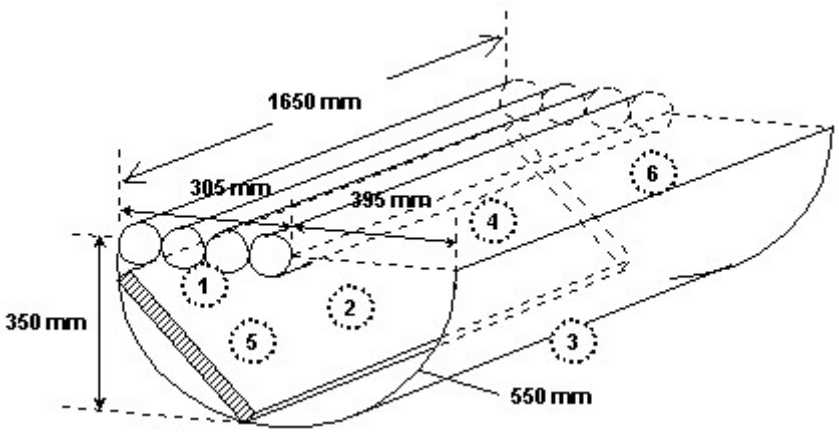

Figure 4. Schematic of the cavity composed by the adsorber and surrounding surfaces.

The temperatures of all surfaces were measured, and they are considered uniform, except those concerning the tubes, because in this case, the upper of the adsorber changes radiant heat directly with the sky while the lower face changes radiant heat with the different surfaces composing the cavity.

3.1. Heat transfer equations

Taking into account the symmetry of the physic problem, the energy equation for the half of the adsorber plate can be expressed in a simple form by:

$$m_p Cp_p \frac{\partial T_p}{\partial t} = 2\left\{4\pi D_t L_t \left[h\left(T_p - T_{ac}\right) + h_V\left(T_p - T_{amb}\right)\right] + h_{r,p-sky}\left(T_p - T_{sky}\right) + Q_{r,i}\right\} \quad (1)$$

where mp is the mass of the tubes, Cp_p the specific heat, T_p the temperature, D_t the diameter, L_t the length, h is the conductance at the interface tube-adsorbent, T_{ac} the activated carbon temperature, h_V the convection coefficient due to wind, T_{amb} the ambient temperature, $h_{r,p\text{-}sky}$ an equivalent radiation coefficient and $Q_{r,i}$ the net radiant heat interchanged with the surfaces composing the cavity. The equivalent sky temperature (T_{sky}) is given by:

$$T_{sky} = \varepsilon_{sky}^{1/4} T_{amb} \quad (2)$$

where ε_{sky} is the apparent emittance of clear sky, given as a function of the dewpoint temperature (T_{dp}, in ^{o}C), according the following equation given by Berdhal and Martin (1984):

$$\varepsilon_{sky} = 0{,}711 + 0{,}56\left(\frac{T_{dp}}{100}\right) + 0{,}73\left(\frac{T_{dp}}{100}\right)^2 \quad (3)$$

The net radiant flux $Q_{r,i}$ (= Q_1) is determined by the "net-radiation method", based on the Poljak's model (Siegel and Howell, 1992), in which the radiant energy transferred to each surface (Q_j) by convection and conduction is equivalent to the net radiation from this surface, as result of the interchange between all surfaces of the cavity. This energy balance can be written as:

$$Q_j = A_j \frac{\varepsilon_j}{1-\varepsilon_j}\left(\sigma T_j^4 - Q_{o,j}\right) = A_j\left(Q_{o,j} - \sum_{k=1}^{N} F_{j-k}\, Q_{o,k}\right) \quad (4)$$

where A_j is the area of surface j, σ the Stephan-Boltzmann constant, ε_j the emittance of the surface j, N the number of surfaces, $F_{j\text{-}k}$ the view factor for the radiant exchange between surfaces j and k, $Q_{o,j}$ the radiant energy leaving surface j, and $Q_{o,k}$ the radiant energy leaving surface k and reaching surface j. All surfaces are considered gray and diffuse, then $\alpha(T) = \varepsilon(T)$.

In order to simplify the calculations, we neglect surfaces 5 and 6 (Fig. 4) placed in the extremities of the cavity. Thus, to determine the net radiant flux from each surface, we have a bidimensional problem, as shown in Fig. 5.

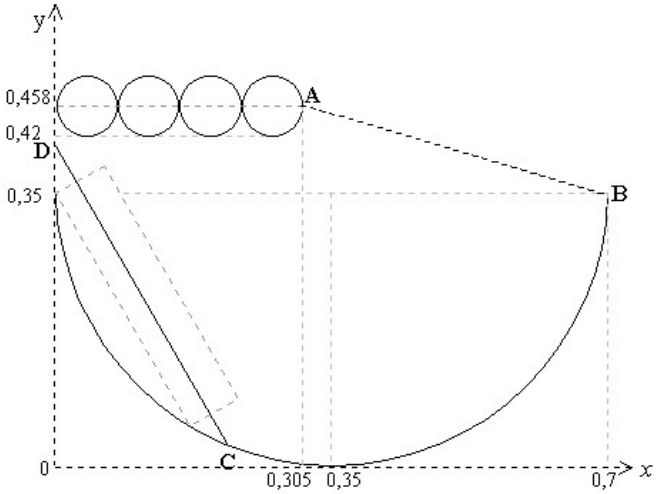

Figure 5. Schematic of the cavity considered for calculating the radiant interchanges.

The set of equations representing the radiant interchange between the surfaces indicated in Fig. 5 can be written as:

$$\frac{Q_1}{A_1}\left[\frac{1}{\varepsilon_1} - F_{11}\frac{1-\varepsilon_1}{\varepsilon_1}\right] - \frac{Q_2}{A_2}F_{12}\left(\frac{1-\varepsilon_2}{\varepsilon_2}\right) - \frac{Q_3}{A_3}F_{13}\left(\frac{1-\varepsilon_3}{\varepsilon_3}\right) - \frac{Q_4}{A_4}F_{14}\left(\frac{1-\varepsilon_4}{\varepsilon_4}\right) =$$

$$= F_{12}\sigma(T_1^4 - T_2^4) + F_{13}\sigma(T_1^4 - T_3^4) + F_{14}\sigma(T_1^4 - T_4^4) \tag{5}$$

$$-\frac{Q_1}{A_1}F_{21}\left(\frac{1-\varepsilon_1}{\varepsilon_1}\right) + \frac{Q_2}{\varepsilon_2 A_2} - \frac{Q_3}{A_3}F_{23}\left(\frac{1-\varepsilon_3}{\varepsilon_3}\right) - \frac{Q_4}{A_4}F_{24}\left(\frac{1-\varepsilon_4}{\varepsilon_4}\right) =$$

$$= F_{21}\sigma(T_2^4 - T_1^4) + F_{23}\sigma(T_2^4 - T_3^4) + F_{24}\sigma(T_2^4 - T_4^4) \tag{6}$$

$$-\frac{Q_1}{A_1}F_{31}\left(\frac{1-\varepsilon_1}{\varepsilon_1}\right) - \frac{Q_2}{A_2}F_{32}\left(\frac{1-\varepsilon_2}{\varepsilon_2}\right) + \frac{Q_3}{A_3}\left[\frac{1}{\varepsilon_3} - F_{33}\frac{1-\varepsilon_3}{\varepsilon_3}\right] - \frac{Q_4}{A_4}F_{34}\left(\frac{1-\varepsilon_4}{\varepsilon_4}\right) =$$

$$= F_{31}\sigma(T_3^4 - T_1^4) + F_{32}\sigma(T_3^4 - T_2^4) + F_{34}\sigma(T_3^4 - T_4^4) \tag{7}$$

$$-\frac{Q_1}{A_1}F_{41}\left(\frac{1-\varepsilon_1}{\varepsilon_1}\right) - \frac{Q_2}{A_2}F_{42}\left(\frac{1-\varepsilon_2}{\varepsilon_2}\right) - \frac{Q_3}{A_3}F_{43}\left(\frac{1-\varepsilon_3}{\varepsilon_3}\right) + \frac{Q_4}{\varepsilon_4 A_4} =$$

$$= F_{41}\sigma(T_4^4 - T_1^4) + F_{42}\sigma(T_4^4 - T_2^4) + F_{43}\sigma(T_4^4 - T_3^4) \tag{8}$$

The areas were obtained from the coordinates of points A, B, C and D, to be: A_1 = 0.48 m^2, A_2 = 0.44 m^2, A_3 = 0.69 m^2 and A_4 = 0.41 m^2. The view factors are indicated in Table 1. The values assumed for the emittance are: ε_1 = 0.95, ε_2 = 0.88, ε_3 = 0.20 and the apparent emittance of the sky (ε_4) was calculated by Eq. (3) at each hour, ranging from 0.86 to 0.89.

The equations system represented by Eqs. (5) to (8) was solved by using the inverse matrix method, from experimental measurements of the surfaces temperatures and meteorological parameters, such as the ambient temperature, wind velocity and humidity, carried out during a typical clear sky day.

Table 1. Bidimensional view factors for the radiant exchange.

Surface	$\mathbf{F_{1-j}}$	$\mathbf{F_{2-j}}$	$\mathbf{F_{3-j}}$	$\mathbf{F_{4-j}}$
1 - tubes	0.356	0.350	0.211	0.018
2 – TIM cover	0.322	0	0.233	0.307
3 - reflectors	0.305	0.364	0.154	0.675
4 - sky	0.017	0.286	0.402	0
Total	1	1	1	1

4. Results and discussion

Table 2 shows the results from calculations of the hourly net radiant heat ($Q_{r,i}$) emitted or received by each surface of the cavity indicated in Fig. 5. The considered period (15 p.m. to 4 a.m.) was defined from experimental data, according to Leite et al. (2005a, 2005b), i.e., the period between the end of the regeneration and the end of the adsorption. The indicated times represent a centered hour.

Table 2. Hourly net radiant heat fluxes.

Time	$\mathbf{Q_{r,1}}$ **(W)**	$\mathbf{Q_{r,2}}$ **(W)**	$\mathbf{Q_{r,3}}$ **(W)**	$\mathbf{Q_{r,4}}$ **(W)**
15:00	1.15	-34.85	-1.02	34.72
16:00	-4.34	-14.79	-2.35	21.49
17:00	-2.78	-12.58	-2.84	18.19
18:00	-3.04	-9.07	-3.01	15.11
19:00	-3.26	-6.11	-2.47	11.84
20:00	-23.15	5.35	-0.40	18.21
21:00	-16.51	0.98	-1.00	16.52
22:00	-11.12	0.21	-1.39	12.29
23:00	-11.23	-2.56	-2.16	15.95
24:00	-8.13	-4.91	-2.76	15.80
01:00	-6.98	-5.79	-3.39	16.16
02:00	-5.93	-6.25	-3.11	15.29
03:00	-4.49	-7.89	-3.33	15.71
04:00	-5.00	-7.18	-2.76	14.94

Based on average values obtained over the whole calculation period, the radiation emitted by the tubes (surface 1) that attains the TIM cover (surface 2) represents 35%, while that that reaches directly the reflector (surface 3) is about 21%. Only 2% traverses directly the aperture (surface 4), and about 57% from the total emitted by surface 1 reaches itself. The radiant energy that passes through the aperture after hitting the reflector represents 14% of the total emitted by the tubes.

The total heat released from the upper side of the adsorber by radiative exchanges with the sky corresponds to 75% of the total heat dissipated from it. Concerning only the losses by radiation, the upper side is responsible for 82% of the total.

5. Conclusion

The radiant heat exchanges from an adsorber-solar collector operating with activated carbon-methanol, as a component of an autonomous icemaker was analized. The energy equation for the adsorber, as well as the equations system concerning the thermal radiation transfers between the adsorber and the surrounding surfaces are presented and solved, by the net-radiation method. The results from calculations have shown that the heat released from the adsorber by radiation is the main mechanism of thermal dissipation during the adsorber cooling and the adsorption process, representing 75% of the total heat losses. It was also demonstrated that about 18% of the net radiant flux is due to the interchange between the under side of the tubes and the surrounding surfaces.

6. Acknowledgements

The authors gratefully acknowledge the Brazilian agency, National Council of Scientific and Technological Development - CNPq, for the financial support provided to this work through Research Project Grant N^{o} 5201673/03-2.

7. References

Berdahl, P. and Martin, M., 1984, "Emissivity of Clear Skies", Solar Energy, Vol.32, N^{o}5, pp. 663-664.

Boubakri, A., 2003, "A New Conception of an Adsorptive Solar-Powered Ice Maker", Renewable Energy, Vol.28, pp. 249-263.

Chinnapa, J.C.V., 1962, " Performance of an Intermittent Refrigerator operated by a Flat-Plate Collector", Solar energy, Vol.6, pp. 143-150.

Critoph, R., Tamainot-Telto, Z. and Munyebvu, E., 1997, "Solar Sorption Refrigerator", Renewable Energy, Vol.12, N^{o}4, pp. 409-417.

Grenier, Ph., Guilleminot, J.J., Meunier, F. and Pons, M., 1988, "Solar Powered Solar Adsorption Cold Storage", Solar Energy Engng., Vol.110, pp. 308-315.

Hildebrand C., Dind, Ph., Pons, M. and Buchter, F., 2004, "A New Solar Power Adsorption Refrigerator with High Performance, Slar Energy, Vol.77, pp. 311-318.

Leite, A.P.F., 1998, "Thermodynamic Analysis and Modelling of an Adsorption-Cycle System for Refrigeration from Low-Grade Energy Sources", Journal of the Brazilian Society of Mech. Sci., Vol.20, pp. 301-324.

Leite, A.P.F., Grilo M.B., Andrade R.R.D. and Belo F.A., 2004, "Dimensioning, Thermal Analysis and Experimental Heat Loss Coefficients of an Adsorptive Solar Icemaker", Renewable Energy, Vol.29, pp. 1643-1663.

Leite, A.P.F., Grilo M.B., Andrade R.R.D., Belo F.A. and Meunier, F., 2005a, "Experimental Evaluation of a Multi-Tubular Adsorber operating with Activated Carbon-Methanol", Adsorption - J. of Int. Adsorption Society, Vol. 11, pp. 543-548.

Leite, A.P.F., Grilo M.B., Andrade R.R.D., Belo F.A. and Meunier, F., 2005b, "An Improved Multi-Tubular Solar Collector Applied to Adsorption Refrigeration", In (to appear): Proc. ISES 2005 Solar World Conference, 6-12 August, Orlando Florida, USA.

Li, M., Wang, R.Z., Xu, Y.X. and Dieng, A.O., 2002, " Experimental Study on Dynamic Performance Analysis of a Flat-Plate Solar Solid-Adsorption Refrigeration for Ice Maker", Renewable Energy, Vol.27, N^{o}2, pp. 211-221.

Meunier, F., 1998, "Solid Sorption Heat Powered Cycles for Cooling and Heat Pumping Applications", Applied Thermal Engng, Vol.98, pp. 715-729.

Siegel, R. and Howell, J.R., 1992, "Thermal Radiation Heat Transfer", 3rd Ed. Taylor & Francis Pub., Washington, USA.

Spinner, B., Goetz, V., Mazet, N., Mauran, S. and Sitou, D., 1999, "Performance of Chemical Reaction Heat Processes coupled to a Solar Source", Journal of Physics IV, Vol.9, pp. 355-360.

8. Responsibility notice

The authors are the only responsible for the printed material included in this paper.